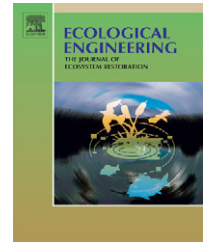


available at [www.sciencedirect.com](http://www.sciencedirect.com)journal homepage: [www.elsevier.com/locate/ecoleng](http://www.elsevier.com/locate/ecoleng)

# GIS-based modeling of spawning habitat suitability for walleye in the Sandusky River, Ohio, and implications for dam removal and river restoration

Daniel Gillenwater<sup>a</sup>, Timothy Granata<sup>a,\*</sup>, Ulrike Zika<sup>b</sup>

<sup>a</sup> The Ohio State University, Department of Civil and Environmental Engineering and Geodetic Science, 2070 Hitchcock Hall, Columbus, OH 43210, United States

<sup>b</sup> The Ohio State University, Department of Civil and Environmental Engineering and Geodetic Science, Aquatic Ecology Laboratory, 232 Research Center, 1314 Kinear Road, Columbus, OH 43212, United States

## ARTICLE INFO

### Article history:

Received 30 June 2005

Received in revised form

4 August 2006

Accepted 10 August 2006

### Keywords:

HSI modeling

Walleye

Dam removal

River restoration

GIS

Habitat modeling

## ABSTRACT

The Sandusky River (Ohio, USA) is the subject of a controversial river restoration proposal involving the removal of a high-head dam to give walleye (*Sander vitreus*) access to upstream spawning areas. Habitat suitability index (HSI) models can add useful information for making such environmental decisions. In this work, a one-dimensional hydraulic river model is coupled with a collection of GIS routines programmed into the ArcGIS® interface for calculating spatial distributions of depth, velocity, and spawning habitat suitability for walleye in a section of the river. The model is evaluated against *in situ* measurements of depth, velocity, and egg density. Results indicate that the model is accurate at predicting depths, but velocity predictions are generally lower than measured in the field. Despite this limitation, egg densities display a significant positive correlation with HSI ( $R^2 = 0.19$ ,  $P = 0.036$ ), indicating that the model can give a general idea of spawning habitat suitability in the river. The model results indicate that the habitat suitability in the river, and hence reproductive success, is dependent on discharge. Habitat suitability is maximized at discharges of 20–25 m<sup>3</sup>/s. Flood events with discharges over 100 m<sup>3</sup>/s reduce the amount of highly suitable habitat in the river to less than 1% of the total area.

© 2006 Elsevier B.V. All rights reserved.

## 1. Introduction

The habitat requirements of a species are the abiotic components of the environment necessary for survival (Rosenfeld, 2003). Loss of habitat is a major factor contributing to the decline of fisheries in both marine and freshwater systems around the world (Langton et al., 1996). In Lake Erie, habitat loss and degradation has been identified as one of the three major problems facing fish and wildlife populations (EPA, 2002). A recent study in the Lake Erie watershed found

fish habitat in many tributaries, shoreline areas, and wetlands to be impaired (EPA, 2002). One Lake Erie tributary that is facing fish habitat loss issues is the Sandusky River in northern Ohio. The river is a major spawning run for several fish species, but a high-head dam at approximately river kilometer (rkm) 29 blocks any migration past this point and the habitat remaining below the dam has become degraded over the years since the dam was built in the early 20th century. There is a hotly debated proposal to remove the dam to restore the Sandusky River ecosystem. In this instance, the ability to quantify habi-

\* Corresponding author at: BPRC, Ohio State University, Columbus, OH, United States. Tel.: +1 614 292 5040; fax: +1 614 292 3780.

E-mail address: [granata.6@osu.edu](mailto:granata.6@osu.edu) (T. Granata).

0925-8574/\$ – see front matter © 2006 Elsevier B.V. All rights reserved.

doi:10.1016/j.ecoleng.2006.08.003

tat quality and quantity under different scenarios becomes essential in making a decision on ecosystem restoration alternatives.

Government agencies have realized the necessity of habitat in maintaining sustainable fisheries and have enacted legislation to combat the loss and destruction of important habitat areas. The Fishery Conservation Act of 1976 called for habitat issues to be included in all fisheries management plans (Fluharty, 2000). The Sustainable Fisheries Act (SFA) of 1996 specified the long-term protection of essential fish habitat (EFH), defined as “those waters and any substrate necessary to fish for spawning, breeding, feeding, or growth to maturity” (SFA, Sec. 3(25), cited in Fluharty, 2000).

A tool to aid in the delineation of important habitat areas and to facilitate the decision making process for environmental management and ecosystem restoration is habitat suitability index (HSI) modeling. Habitat suitability index models were originally developed in the 1970s by the US Fish and Wildlife Service (USFWS) as a part of their Habitat Evaluation Procedures (HEP). The HEP system was developed to determine the quality and quantity of habitat for a given species to assess the impacts of human activities on fish and wildlife populations (USFWS, 1980). Brown et al. (2000) describe some of the various management applications of HSI modeling as: (1) evaluating the impacts of regulatory alternatives, specifically for EFH studies, (2) identifying and prioritizing areas for conservation actions, and (3) ascertaining the potential impacts of environmental change. HSI models may also be used to guide ecosystem restoration activities by indicating the physical habitat conditions that should be created to benefit target organisms.

The HSI itself is a value derived from key habitat components of a selected species or life history stage (USFWS, 1980). The key habitat components are described by suitability curves on a scale from 0 to 1 over a range of values for the habitat variable. The composite HSI value for a given area is obtained by mathematically combining the individual suitability values of the habitat components to give an overall index of habitat suitability on a scale of 0–1.

One of the original HSI models is the Physical Habitat Simulation System (PHABSIM), which was developed by the US Geological Survey (USGS) as part of the Instream Flow Incremental Methodology (Bovee et al., 1998). PHABSIM consists of a suite of computer programs to: (1) model the spatial distribution of hydraulic variables, such as depth and velocity, throughout the study reach, (2) determine the spatial distribution of habitat suitability, and (3) relate the overall suitability of the study reach to discharge (Waddle, 2001). PHABSIM is a very specialized software package that contains its own hydraulic modeling software, HSI calculation routines, and mapping software.

In recent years, several new developments in HSI modeling in rivers have emerged that improved upon the original PHABSIM design for use in ecological engineering and restoration studies (Spence and Hickley, 2000; Bockelmann et al., 2004). Probably the most notable advance has been the coupling of two-dimensional hydraulic river models with HSI models to simulate depth and velocity (Ghanem et al., 1996; Leclerc et al., 1996; Tiffan et al., 2002; Bockelmann et al., 2004; Korman et al., 2004). These models have the advantage of not needing empirical data on water velocity distributions to calculate

bed roughness for velocity simulations at different discharges. Also, since two-dimensional hydraulic models simulate velocity distributions throughout a reach via a series of cells, the practice of modeling long lengths of a stream reach as a single cross section can be avoided. One-dimensional hydraulic models have several advantages including: (1) the need of only two boundary conditions (upstream discharge, downstream water level), (2) they are simple to calibrate compared to two-dimensional models, and (3) they are commonly used commercially for other river applications.

HSI modeling has also become common in other aquatic ecosystems. Several investigators have used HSI modeling to determine areas of optimal fish habitat in oceans, bays, estuaries, and lakes to support essential fish habitat decision making (Rubec et al., 1998; Brown et al., 2000; Eastwood et al., 2001; Rowe et al., 2002). In all of these situations, the entire HSI modeling process takes place using a commercially available geographic information system (GIS).

GIS has been used for many different tasks in fishery biology that involve a spatial dimension, including mapping fish habitats and fish distributions, determining the effects of land use on fish populations, and analyzing spatial and temporal changes in fish distribution (Fisher and Rahel, 2004). HSI modeling is one of the newer fields to use GIS.

GIS are well suited for HSI modeling for several reasons. These systems can overlay layers representing the spatial distribution of different environmental variables in either raster or vector format. GIS has the ability to perform spatial operations on the different layers of data, using either the suite of built-in functions or those that are user defined. Many of these commercially available systems, such as ArcGIS®, can be customized to create programs to automate data analysis routines too cumbersome to perform manually. Finally, GIS is widely available and is a ubiquitous component of almost every state level fishery biologist's software arsenal.

Despite the obvious advantages of GIS for HSI modeling, its use in river systems is scant. The most likely explanation is the requirement that a river HSI model must be coupled with a hydraulic model to determine the spatial distribution of depths and velocities. This coupling can create complications with data transfers between the two software components. To this date there is only one example of a GIS being used for this purpose. Tiffan et al. (2002) linked a two-dimensional hydraulic model of a river with a GIS-based logistic regression model of habitat suitability for Chinook salmon.

To our knowledge, no merger between a one-dimensional hydraulic river model and a GIS-based habitat model has been published. This concept is intriguing because one-dimensional river models are far more abundant and commonly used than two-dimensional models. However, one-dimensional models are only able to give an average depth and velocity for a river cross section. Therefore, in addition to calculating the spatial distribution of HSI, the GIS is needed to determine the spatial distribution of depth and velocity throughout the reach.

### 1.1. Study objectives

The goal of this study is to couple an existing one-dimensional river model with a GIS-based software package to determine

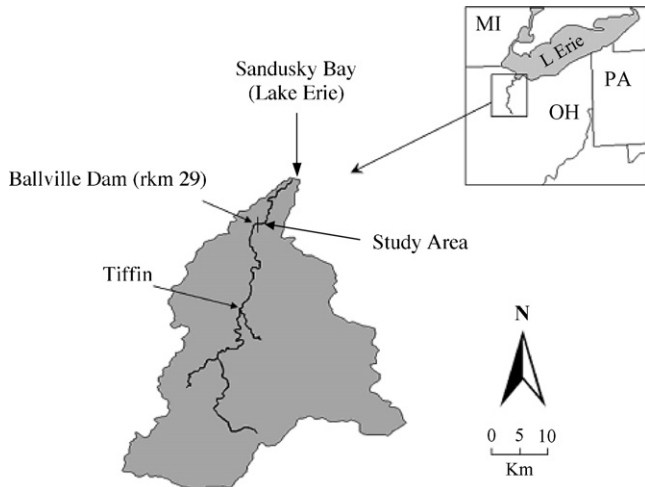


Fig. 1 – Map of the Sandusky River watershed.

the spatial distributions of depth and velocity throughout the study reach, as well as the distribution of habitat suitability for walleye (*Sander vitreus*) spawning. In this work, the following specific objectives will be addressed:

- (1) To develop a habitat suitability model that it is user-friendly and can be transferred to other river systems in an ArcGIS V 9.0 format.
- (2) To produce GIS maps of habitat suitability and record the total availability of habitat for the study reach for each time step of the hydraulic model.
- (3) To validate the model using *in situ* data on depth, velocity, and egg density collected during the 2004 spawning season in the Sandusky River.

If reliable, the results of this model will help to determine how river conditions during a given spawning season could potentially impact walleye reproductive success for that year.

## 2. Study area and species

### 2.1. Study area

This study was carried out on the Sandusky River, a tributary to Lake Erie in north-central Ohio (Fig. 1). The river is 210 km in length and drains an area of approximately 3700 km<sup>2</sup> (SRWC, 2002). The watershed receives an average of 93 cm of rain a year, 30% of which drains directly into surface waters (SRWC, 2002). Ninety-eight percent of the river is considered Warm Water Habitat (WWH) by the Ohio Environmental Protection Agency's (OEPA) Aquatic Life Use Standards, meaning it provides average assemblages of fish and invertebrates found in reference streams in the eco-region. However, siltation is a large threat to spawning habitat (SRWC, 2002).

There are currently four dams on the Sandusky River. The first and largest of these is the Ballville Dam, located near Fremont, Ohio, at rkm 29. Gravel is the preferred spawning substrate of walleye but it is severely limited downstream of this dam. The Ballville Dam restricts fish from moving upstream

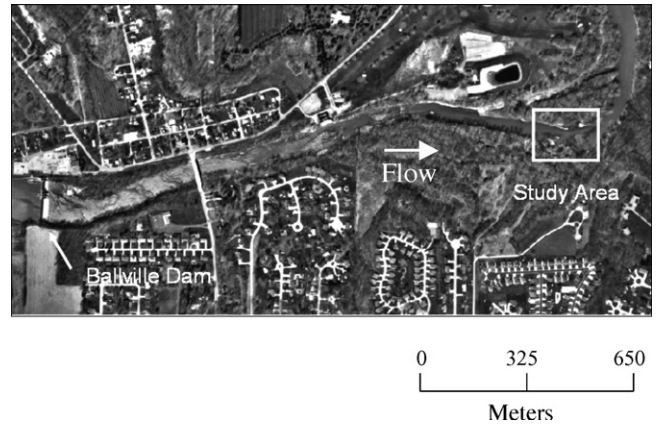


Fig. 2 – Aerial photograph of the Sandusky River between river kilometer (rkm) 29 and 27 showing the location of the study area relative to the Ballville Dam.

to additional gravel beds, which are estimated to have a combined area of 654 000 m<sup>2</sup> (Cheng et al., 2006). Another problem is that flood control structures created in the early 1970s in downtown Fremont have caused siltation downstream of the dam, which destroyed several gravel beds in that area (Tea, 1999). The combination of passage blockage by the dam and habitat destruction has restricted the Sandusky River walleye population to spawning on a single gravel bed of approximately 64 000 m<sup>2</sup> in area (Cheng et al., 2006). This loss of habitat has been implicated in the decline of the walleye spawning population in the river (Tea, 1999).

The model was developed, tested, and validated on a 200 m reach located at rkm 27, approximately 2 km downstream of the Ballville Dam (Figs. 1 and 2). This study area was chosen because it contains a variety of different hydraulic habitat types (riffles, runs, pools) as well as the only remaining major gravel bed and walleye spawning ground in the Sandusky River. The floodplain in the study area is relatively flat, but crossed by abandoned river channels on both sides. It has a densely forested canopy with a well-developed understory.

### 2.2. Walleye

Walleye are abundant in the Western Basin of Lake Erie, where they are one of the most important recreational and commercial fish species (Leach and Nepszy, 1976). Adult walleye spend the majority of their lives in the lake. However, when the spawning season begins in the early spring, a portion of the Western Basin stock migrates into the Sandusky and Maumee Rivers to spawn (Regier et al., 1969). Walleye exhibit strong homing behavior for their natal spawning grounds (Crowe, 1962; Jennings et al., 1996) and molecular evidence indicates that the spawning stocks of the Maumee and Sandusky rivers are genetically different (Merker and Woodruff, 1996) indicating that walleye are unlikely to seek new spawning tributaries if conditions in their natal waterbody deteriorate.

Walleye spawning runs usually occur between water temperatures of 4–11 °C (Eschmeyer, 1950). They are broadcast spawners, meaning that they freely deposit their eggs over the substrate and provide no parental care (Eschmeyer, 1950;

Ellis and Giles, 1965). Despite this fact, walleye display a strong preference for spawning over gravel and cobble substrates (Eschmeyer, 1950; Armstrong and Dyke, 1967; Stepaniuk, 1989).

### 3. Methods

#### 3.1. Input data

The channel and floodplain were surveyed to create a digital elevation model (DEM) of the river. The channel was surveyed using a Trimble™ 5700 GPS receiver (accurate to  $\pm 1$  cm horizontally and vertically) equipped with a Trimble Zephyr antenna, mounted on a range pole. The receiver was set to collect data at 1 Hz in static occupation mode. A local base station was set up in a nearby field using a Trimble 5700 GPS receiver equipped with a Novatel™ 600 GPS antenna. Surveying was performed by starting at one side of the bank and slowly walking across to the other bank, keeping the base of the range pole in constant contact with the river bed. The river was traversed in a zig-zag fashion with the starting points on each bank no more than 6 m apart. Surveying took place on 26 July 2003.

GPS data were processed using Trimble Geomatics Office™ software. Data were converted from static occupation to continuous mode and referenced to the local base station. The position of the local base was determined by referencing its position to the Ohio Department of Transportation's base station in Tiffin, Ohio. ArcScene™ was later used to eliminate erroneous data points.

It was impossible to survey the floodplain with GPS because the dense tree canopy caused a high degree of backscatter in the GPS signal. Surveying in this area was performed using a Sokkia™ SET 5E Total Station. A closed traverse method (Bannister et al., 1998) was employed. Temporary benchmarks for horizontal and vertical survey control were established using the Trimble 5700 in areas without dense tree cover. The area was surveyed by taking measurements at breaks in the topography of the terrain so that all important landforms were included. Surveying took place on 3 September, 1 October, 5 October, and 10 November 2004.

The width of the surveyed area on the north floodplain extended from the river bank to an artificial levee constructed adjacent to the River Cliff Golf Course (approximately 100 m). On the south floodplain, the width extended from the river bank to a natural ridge that ran parallel to the river (approximately 100 m). Elevations on top of the ridge were obtained from a USGS topographic map. There were several islands in the study area with tree cover that were also surveyed using the total station. Raw survey data were later reduced with the help of a licensed professional to assure that the required level of accuracy was obtained.

A digital elevation model (DEM) of the river and floodplain was created from the GPS and total station surveys. Elevation points were input into ArcMap™ and a Triangulated Irregular Network (TIN) was created. The TIN was then converted to a raster layer with a  $3\text{ m} \times 3\text{ m}$  cell size. A separate DEM of the river bed was created from the survey points within the channel using the same method.

Bed roughness was used to calibrate velocities throughout the study reach. This was accomplished using a modification of the method of Bovee and Milhous (1978), in which roughness is back calculated from field measurements of depth, velocity, and bed slope.

Water depths and velocities were measured on 2 September 2004 ( $Q = 15\text{ m}^3/\text{s}$ ) throughout the study reach using two different methods. In deep areas ( $>0.45\text{ m}$ ) the measurements were made using a Sontek® acoustic Doppler profiler (ADP) with bottom tracking and GPS to achieve a more continuous transect of velocity and depth for each cell of the HSI model (see Section 3.2). The ADP system was mounted on a canoe and linked with the Trimble 5700 GPS to determine the location. The ADP collected data at 1 Hz and averaged data over 5 s. The GPS position corresponded to the location of the last velocity measurement in the 5-s average. The canoe was maneuvered across the width of the channel in a zig-zag fashion, attempting to keep the endpoints of the transects no further than 6 m apart on each river bank. The canoe was maneuvered slowly ( $\sim 0.3\text{ m/s}$ , measured with bottom tracking) so the distance that the velocity measurements were averaged across was as short as possible.

In shallower areas ( $<0.45\text{ m}$ ), velocity was measured using a hand-held FlowTracker™ acoustic Doppler velocimeter (Sontek Inc.). The FlowTracker collected data at 1 Hz and averaged velocity measurements over 30 s. At each sampling point, the depth was measured with a depth stick and the average velocity was determined from at 60% of the total depth, based on a log-velocity distribution (Chapra, 1997). The position of each sampling point was marked with the GPS. The maximum distance between sampling points was approximately 6 m.

The bed roughness coefficient, Manning's  $n$ , was determined at each point by rearranging the Manning's equation for velocity:

$$n = \frac{d^{2/3} \times S_0^{1/2}}{u} \quad (1)$$

where  $d$  is the depth (m),  $S_0$  the bed slope, and  $u$  is the velocity (m/s) downstream direction.

A spatially interpolated raster layer of bed roughness in the study area was created from the point values of Manning's  $n$  using an Inverse Distance Weighted (IDW) interpolation method using the Spatial Analyst extension in ArcMap. The roughness values for the floodplains were determined by visual inspection and comparison to reference floodplains in Arcement and Schneider (1989). Substrate maps in the study area were provided by the Ohio Department of Natural Resources (ODNR), Geological Survey and modified where necessary based on field observations.

The three most important habitat variables for spawning walleye are depth, velocity, and substrate. The suitability curves from the Saskatchewan Fisheries Laboratory in Canada (Liaw, 1991) for these variables were used in the model.

#### 3.2. Model development

Two separate software systems were integrated for the HSI model: an existing hydraulic model of the Sandusky River and the new GIS-based system. Fig. 3 shows the different compo-

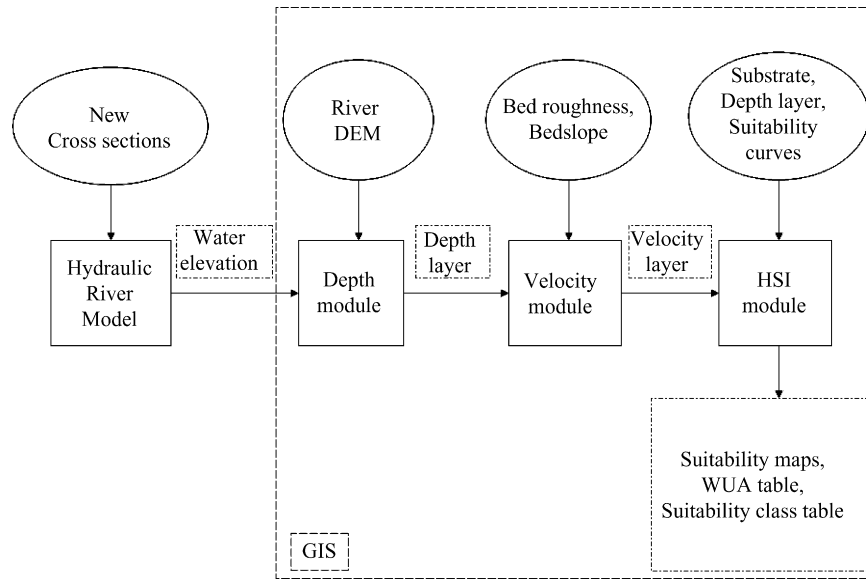


**Fig. 3 – Flow diagram of the various model components (solid squares) and their associated input (ovals) and output (dashed squares) data. All modules within the GIS box are routines carried out by the GIS software.**

nents of this coupled system and the interactions between them.

The hydraulic model of the Sandusky River was developed by Cheng (2001) using Mike 11™ one-dimensional river modeling software. The upstream boundary of the model was set in Tiffin, Ohio, and the downstream boundary was Lake Erie (Fig. 1). The model was driven at the upstream end using discharge data obtained from the USGS gaging station near Fremont, Ohio (USGS gage 04198000), and weighted by watershed area to the Tiffin boundary. At the downstream boundary, the model was driven with water level data from the National Oceanographic and Atmospheric Administration (NOAA, 2006) water level station at Marblehead, Ohio.

The model was modified with additional river cross sections from the surveys of the study area to accurately predict the water surface elevation at various discharges. The DEM of the river and floodplain was loaded into MikeGIS™, an ArcView™ interface with Mike 11 that aids in model development and flood mapping. Three cross-sections of the river and the floodplain were extracted from the DEM at approximately equal distances and imported into the existing river model. To calibrate the model, predicted water surface elevations were compared to those measured in the field and adjustments in channel roughness (*n*) were made for each cross section.

The GIS software package was programmed in Visual Basic® using ArcObjects™. Three independent software modules were designed with graphical user interfaces (GUIs) to perform each of the tasks in the model: mapping the distributions of (1) depth, (2) velocity, and (3) HSI. Each module allows the user to select the input data, and the locations for the output files. The individual modules are described below.

### 3.2.1. Depth module

After running the hydraulic model for the desired time series, the first task for the GIS model is to create a raster layer of

the depths throughout the study area for each time step. The module uses the DEM of the river bottom and the time series of water surface elevations from the hydraulic model and determines the water depth in each raster cell by subtracting the bottom elevation from the water surface elevation. Water surface elevations were linearly interpolated between cross sections.

### 3.2.2. Velocity module

Next, raster layers of the velocity in each model cell are created for each time step. The module uses the cell depth raster layers and the Manning's *n* layer and determines the water velocity in each cell using the Manning equation:

$$u = \frac{d^{2/3} \times S_o^{1/2}}{n} \tag{2}$$

where the variables are the same as those listed in Eq. (1).

### 3.2.3. HSI module

Last, depth and velocity values are converted to their corresponding suitability values and the overall HSI is calculated for each cell. The module uses the velocity and depth layers, and the suitability curves for these variables, to create layers of depth and velocity suitability for each time step. It assigns the depth and velocity predictions a suitability value: unsuitable (0), low (0.2), moderate (0.6), or high (1). The suitability curves used are from the Saskatchewan Fisheries Laboratory. A pre-existing layer of substrate suitability is also used, however the values remain static as the substrate is assumed to remain constant over time. The program then computes the overall HSI value for each grid cell as the geometric mean of the three suitability values:

$$HSI = (I_v \times I_d \times I_s)^{1/3} \tag{3}$$

where  $I_v$  is the velocity suitability index,  $I_d$  the depth suitability index, and  $I_s$  is the substrate suitability index.

In addition to creating maps of overall HSI for each time step of the model, the HSI module also calculates the weighted usable area (WUA) (Bovee et al., 1998) of habitat in the study reach, quantified as:

$$WUA = A_i \times C_i \quad (4)$$

where  $A_i$  is the area of cell  $i$  and  $C_i$  is the HSI value of cell  $i$ .

The WUA provides an index of the overall habitat suitability in a reach of the river for a given discharge. The volumetric discharge,  $Q$ , was measured at the USGS gage. WUA values are output to a database file for the entire simulated time series.

For easier interpretation of the HSI model results the HSI values are grouped into one of four classes (Brown et al., 2000) representing high ( $HSI \geq 0.8$ ), medium ( $0.8 > HSI \geq 0.4$ ), and low ( $0.4 > HSI > 0$ ) suitability, and unsuitable ( $HSI = 0$ ) areas. The HSI module calculates the total area in each suitability class for each time step and outputs the values to a database file.

### 3.3. Validation data

Walleye eggs were collected in the study area during the spring of 2004. Collection began on 26 March when the water temperatures had risen above 4 °C and the Ohio Division of Wildlife creel clerks had reported the presence of female walleye in the river. Sampling continued 3 days a week, weather and flow conditions permitting, until 30 April when the deposition of new eggs in the spawning grounds had ceased and the female walleye catch had declined to zero. Eggs were also collected during the 2003 season for a different project (Gillenwater, 2005), but the sample locations were not marked with GPS. These data were used to estimate the total egg deposition in 2003.

On each sampling day, a minimum of six random egg samples were taken throughout the 200 m reach for a total of 75 samples. The eggs were collected by placing a Surber sampler (30 cm × 33 cm, 500 μm mesh) over the river bottom and agitating the substrate by hand for 1 min. Water depth was measured at all egg sampling locations and velocity was measured at most locations. The positions of the egg samples were determined with the Trimble™ GPS unit. The water depth measurements were made using a meter stick. Velocity measurements were made using the FlowTracker with data averaged them over a 30 s interval. For depths <0.75 m, the average velocity was determined at 60% of the total depth, while at depths ≥0.75 m, it was made at 20% and 80% of the maximum depths, based on a log-velocity distribution (Chapra, 1997). We were unable to measure velocity at all egg sampling locations because the FlowTracker was unavailable on several days during the field season. Discharges during the sampling period ranged from 14 to 46 m<sup>3</sup>/s. The eggs were transported to the laboratory, identified, and determined as alive or dead (Eschmeyer, 1950; McElman and Balon, 1979). The developmental stage of each live egg was determined, based on McElman and Balon (1979).

### 3.4. GIS model calibration and validation

First, the depth and velocity predictions of the model were calibrated to the *in situ* depth and velocity measurements collected on 2 September 2004. The model predictions were compared to the field data using a paired t-test. Second, the model predictions were validated using the *in situ* depth and velocity measurements taken during the 2004 spawning season. The model results for the appropriate day were compared to the *in situ* data using a paired t-test.

Finally, the HSI values predicted by the model were compared to the observed walleye egg densities (no./m<sup>2</sup>) to determine how well the model represented the true spawning habitat suitability. Only cleavage stage embryos (stages C1<sup>1</sup>–C3<sup>3</sup>) were included in this analysis, since the temperature data indicated that these eggs were likely deposited since the previous sampling day. Egg densities were normalized by dividing the individual values by the maximum egg density observed on the sampling day to give a dimensionless index of egg abundance. The normalized egg densities were then regressed against the average depth suitability, velocity suitability, and HSI experienced between sampling days. In addition, the normalized egg densities in each depth and velocity suitability and HSI class (low, moderate, and high suitability, and unsuitable) were compared by a one-way ANOVA test to determine if the differences between the classes were significant. All statistical analyses were carried out in Minitab™ (V 14). The significance level was set at  $\alpha = 0.05$ .

### 3.5. Determination of Sandusky River habitat quality

To determine how the walleye spawning habitat suitability of the Sandusky River varies with discharge, the model was run for a variety of discharges ranging from 5 to 150 m<sup>3</sup>/s. The model was then run for the spawning seasons of 1989–1993, as well as for 2003 and 2004, to assess how spawning habitat suitability varied over time. The time period of 1989–1993 was chosen because daily water temperature data were available from the Fremont water treatment plant for those five consecutive years. For our purposes, we defined the spawning season as beginning on the first day in March when the water temperature reached 4 °C and ending when the 5-day running average temperature (after March) was 11 °C.

## 4. Results

### 4.1. Model calibration and validation

No differences between modeled and measured depths and velocities for the calibration dataset were found (Table 1).

**Table 1 – Calibration statistics for depth and velocity (predicted – measured)**

| Variable | N   | Mean difference ± 1 S.D. (m) | P     |
|----------|-----|------------------------------|-------|
| Depth    | 118 | 0.0015 ± 0.23                | 0.108 |
| Velocity | 115 | −0.007 ± 0.24                | 0.761 |

S.D. = standard deviation.

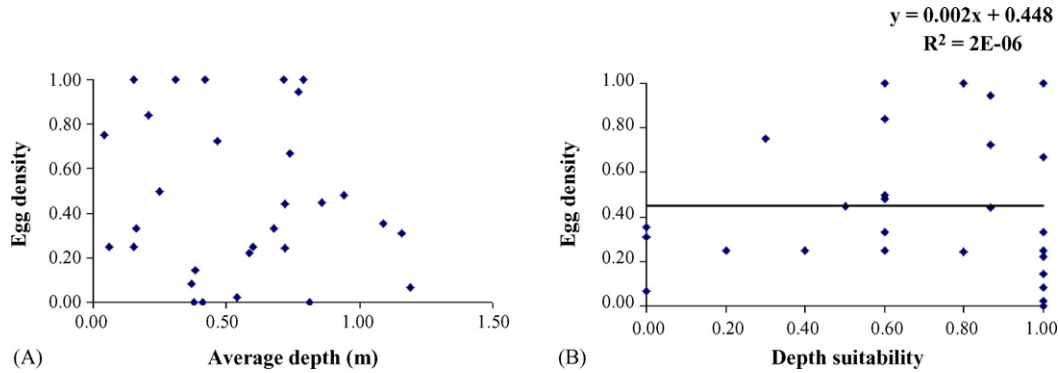


**Fig. 4 – (A) Relationship of normalized egg density to the average model predicted depth and (B) relationship between normalized egg density and the average depth suitability.**

**Table 2 – Validation statistics for depth and velocity (predicted – measured)**

| Variable | N  | Mean difference ± 1 S.D. (m/s) | P     |
|----------|----|--------------------------------|-------|
| Depth    | 33 | 0.002 ± 0.25                   | 0.961 |
| Velocity | 14 | -0.31 ± 0.36                   | 0.007 |

S.D. = standard deviation.

We therefore considered the model successfully calibrated. Also, no difference between modeled and measured depths for the validation dataset was found (Table 2) for the range of discharges simulated (14–46 m<sup>3</sup>/s). However, the modeled velocities were consistently lower than the measured values (Table 2). This was likely due to the complex channel geometry of the study area and the fact that time and safety constraints

only allowed us to collect one velocity calibration dataset at an intermediate discharge. Also, not all of the positions of our sample points correctly processed due to problems with the GPS, which lead to rather small sample sizes for the validation datasets.

No relationship between the average modeled depths during the 1 or 2 days before collection and the normalized egg density was detected (Fig. 4A). There was no significant correlation between the average depth suitability before collection and normalized egg density (Fig. 4B). ANOVA comparisons of normalized egg density and both the average and maximum depth suitability classes experienced before collection showed no significant differences between the egg densities in the different classes (Table 3).

The relationship between the average modeled velocity before collection and the normalized egg density is shown

**Table 3 – Results of analysis of variance on egg density and HSI parameters (p < 0.05)**

| Test   | Source | DF | SS      | MS     | F    | P      |  |       |   |        |        |      |        |       |    |         |        |  |       |   |        |        |      |        |       |    |         |        |  |       |   |        |        |      |        |       |    |         |        |  |       |   |        |        |      |        |       |    |         |        |  |       |   |        |        |      |        |       |    |         |        |                                       |       |   |        |        |      |        |       |    |        |        |                                       |       |   |        |        |      |        |       |    |        |        |                                       |       |   |        |        |      |        |       |    |        |        |                                       |       |   |        |        |      |        |       |
|--|--------|----|---------|--------|------|--------|--|-------|---|--------|--------|------|--------|-------|----|---------|--------|--|-------|---|--------|--------|------|--------|-------|----|---------|--------|--|-------|---|--------|--------|------|--------|-------|----|---------|--------|--|-------|---|--------|--------|------|--------|-------|----|---------|--------|--|-------|---|--------|--------|------|--------|-------|----|---------|--------|---------------------------------------|-------|---|--------|--------|------|--------|-------|----|--------|--------|---------------------------------------|-------|---|--------|--------|------|--------|-------|----|--------|--------|---------------------------------------|-------|---|--------|--------|------|--------|-------|----|--------|--------|---------------------------------------|-------|---|--------|--------|------|--------|-------|
| Egg density vs. average depth suitability class        | Class  | 3  | 0.208   | 0.069  | 0.52 | 0.673  |  |       |   |        |        |      |        |       |    |         |        |  |       |   |        |        |      |        |       |    |         |        |  |       |   |        |        |      |        |       |    |         |        |  |       |   |        |        |      |        |       |    |         |        |  |       |   |        |        |      |        |       |    |         |        |                                       |       |   |        |        |      |        |       |    |        |        |                                       |       |   |        |        |      |        |       |    |        |        |                                       |       |   |        |        |      |        |       |    |        |        |                                       |       |   |        |        |      |        |       |
|  | Error  | 28 | 3.74    | 0.134  |      |        | Egg density vs. maximum depth suitability class        | Class | 3 | 0.262  | 0.131  | 1    | 0.379  | Error | 28 | 3.649   | 0.13   | Egg density vs. average velocity suitability class     | Class | 1 | 0.34   | 0.34   | 2.98 | 0.1    | Error | 19 | 2.164   | 0.114  | Egg density vs. maximum velocity suitability class     | Class | 1 | 0.124  | 0.124  | 1.03 | 0.323  | Error | 20 | 2.416   | 0.121  | Egg density vs. average NEW velocity suitability class | Class | 2 | 0.515  | 0.257  | 2.41 | 0.116  | Error | 19 | 2.026   | 0.107  | Egg density vs. maximum NEW velocity suitability class | Class | 2 | 0.7128 | 0.356  | 3.71 | 0.044* | Error | 19 | 1.18276 | 0.0962 | Egg Density vs. average HSI class     | Class | 2 | 0.318  | 0.159  | 1.4  | 0.271  | Error | 19 | 2.158  | 0.114  | Egg density vs. maximum HSI class     | Class | 2 | 0.34   | 0.17   | 1.57 | 0.233  | Error | 20 | 2.172  | 0.109  | Egg density vs. average NEW HSI class | Class | 3 | 0.7206 | 0.2402 | 2.55 | 0.086  | Error | 19 | 1.7916 | 0.0943 | Egg density vs. maximum NEW HSI class | Class | 2 | 0.9247 | 0.4623 | 5.55 | 0.013* | Error |
| Egg density vs. maximum depth suitability class        | Class  | 3  | 0.262   | 0.131  | 1    | 0.379  |  |       |   |        |        |      |        |       |    |         |        |  |       |   |        |        |      |        |       |    |         |        |  |       |   |        |        |      |        |       |    |         |        |  |       |   |        |        |      |        |       |    |         |        |  |       |   |        |        |      |        |       |    |         |        |                                       |       |   |        |        |      |        |       |    |        |        |                                       |       |   |        |        |      |        |       |    |        |        |                                       |       |   |        |        |      |        |       |    |        |        |                                       |       |   |        |        |      |        |       |
|  | Error  | 28 | 3.649   | 0.13   |      |        | Egg density vs. average velocity suitability class     | Class | 1 | 0.34   | 0.34   | 2.98 | 0.1    | Error | 19 | 2.164   | 0.114  | Egg density vs. maximum velocity suitability class     | Class | 1 | 0.124  | 0.124  | 1.03 | 0.323  | Error | 20 | 2.416   | 0.121  | Egg density vs. average NEW velocity suitability class | Class | 2 | 0.515  | 0.257  | 2.41 | 0.116  | Error | 19 | 2.026   | 0.107  | Egg density vs. maximum NEW velocity suitability class | Class | 2 | 0.7128 | 0.356  | 3.71 | 0.044* | Error | 19 | 1.18276 | 0.0962 | Egg Density vs. average HSI class                      | Class | 2 | 0.318  | 0.159  | 1.4  | 0.271  | Error | 19 | 2.158   | 0.114  | Egg density vs. maximum HSI class     | Class | 2 | 0.34   | 0.17   | 1.57 | 0.233  | Error | 20 | 2.172  | 0.109  | Egg density vs. average NEW HSI class | Class | 3 | 0.7206 | 0.2402 | 2.55 | 0.086  | Error | 19 | 1.7916 | 0.0943 | Egg density vs. maximum NEW HSI class | Class | 2 | 0.9247 | 0.4623 | 5.55 | 0.013* | Error | 19 | 1.5833 | 0.0833 |                                       |       |   |        |        |      |        |       |
| Egg density vs. average velocity suitability class     | Class  | 1  | 0.34    | 0.34   | 2.98 | 0.1    |  |       |   |        |        |      |        |       |    |         |        |  |       |   |        |        |      |        |       |    |         |        |  |       |   |        |        |      |        |       |    |         |        |  |       |   |        |        |      |        |       |    |         |        |  |       |   |        |        |      |        |       |    |         |        |                                       |       |   |        |        |      |        |       |    |        |        |                                       |       |   |        |        |      |        |       |    |        |        |                                       |       |   |        |        |      |        |       |    |        |        |                                       |       |   |        |        |      |        |       |
|  | Error  | 19 | 2.164   | 0.114  |      |        | Egg density vs. maximum velocity suitability class     | Class | 1 | 0.124  | 0.124  | 1.03 | 0.323  | Error | 20 | 2.416   | 0.121  | Egg density vs. average NEW velocity suitability class | Class | 2 | 0.515  | 0.257  | 2.41 | 0.116  | Error | 19 | 2.026   | 0.107  | Egg density vs. maximum NEW velocity suitability class | Class | 2 | 0.7128 | 0.356  | 3.71 | 0.044* | Error | 19 | 1.18276 | 0.0962 | Egg Density vs. average HSI class                      | Class | 2 | 0.318  | 0.159  | 1.4  | 0.271  | Error | 19 | 2.158   | 0.114  | Egg density vs. maximum HSI class                      | Class | 2 | 0.34   | 0.17   | 1.57 | 0.233  | Error | 20 | 2.172   | 0.109  | Egg density vs. average NEW HSI class | Class | 3 | 0.7206 | 0.2402 | 2.55 | 0.086  | Error | 19 | 1.7916 | 0.0943 | Egg density vs. maximum NEW HSI class | Class | 2 | 0.9247 | 0.4623 | 5.55 | 0.013* | Error | 19 | 1.5833 | 0.0833 |                                       |       |   |        |        |      |        |       |    |        |        |                                       |       |   |        |        |      |        |       |
| Egg density vs. maximum velocity suitability class     | Class  | 1  | 0.124   | 0.124  | 1.03 | 0.323  |  |       |   |        |        |      |        |       |    |         |        |  |       |   |        |        |      |        |       |    |         |        |  |       |   |        |        |      |        |       |    |         |        |  |       |   |        |        |      |        |       |    |         |        |  |       |   |        |        |      |        |       |    |         |        |                                       |       |   |        |        |      |        |       |    |        |        |                                       |       |   |        |        |      |        |       |    |        |        |                                       |       |   |        |        |      |        |       |    |        |        |                                       |       |   |        |        |      |        |       |
|  | Error  | 20 | 2.416   | 0.121  |      |        | Egg density vs. average NEW velocity suitability class | Class | 2 | 0.515  | 0.257  | 2.41 | 0.116  | Error | 19 | 2.026   | 0.107  | Egg density vs. maximum NEW velocity suitability class | Class | 2 | 0.7128 | 0.356  | 3.71 | 0.044* | Error | 19 | 1.18276 | 0.0962 | Egg Density vs. average HSI class                      | Class | 2 | 0.318  | 0.159  | 1.4  | 0.271  | Error | 19 | 2.158   | 0.114  | Egg density vs. maximum HSI class                      | Class | 2 | 0.34   | 0.17   | 1.57 | 0.233  | Error | 20 | 2.172   | 0.109  | Egg density vs. average NEW HSI class                  | Class | 3 | 0.7206 | 0.2402 | 2.55 | 0.086  | Error | 19 | 1.7916  | 0.0943 | Egg density vs. maximum NEW HSI class | Class | 2 | 0.9247 | 0.4623 | 5.55 | 0.013* | Error | 19 | 1.5833 | 0.0833 |                                       |       |   |        |        |      |        |       |    |        |        |                                       |       |   |        |        |      |        |       |    |        |        |                                       |       |   |        |        |      |        |       |
| Egg density vs. average NEW velocity suitability class | Class  | 2  | 0.515   | 0.257  | 2.41 | 0.116  |  |       |   |        |        |      |        |       |    |         |        |  |       |   |        |        |      |        |       |    |         |        |  |       |   |        |        |      |        |       |    |         |        |  |       |   |        |        |      |        |       |    |         |        |  |       |   |        |        |      |        |       |    |         |        |                                       |       |   |        |        |      |        |       |    |        |        |                                       |       |   |        |        |      |        |       |    |        |        |                                       |       |   |        |        |      |        |       |    |        |        |                                       |       |   |        |        |      |        |       |
|  | Error  | 19 | 2.026   | 0.107  |      |        | Egg density vs. maximum NEW velocity suitability class | Class | 2 | 0.7128 | 0.356  | 3.71 | 0.044* | Error | 19 | 1.18276 | 0.0962 | Egg Density vs. average HSI class                      | Class | 2 | 0.318  | 0.159  | 1.4  | 0.271  | Error | 19 | 2.158   | 0.114  | Egg density vs. maximum HSI class                      | Class | 2 | 0.34   | 0.17   | 1.57 | 0.233  | Error | 20 | 2.172   | 0.109  | Egg density vs. average NEW HSI class                  | Class | 3 | 0.7206 | 0.2402 | 2.55 | 0.086  | Error | 19 | 1.7916  | 0.0943 | Egg density vs. maximum NEW HSI class                  | Class | 2 | 0.9247 | 0.4623 | 5.55 | 0.013* | Error | 19 | 1.5833  | 0.0833 |                                       |       |   |        |        |      |        |       |    |        |        |                                       |       |   |        |        |      |        |       |    |        |        |                                       |       |   |        |        |      |        |       |    |        |        |                                       |       |   |        |        |      |        |       |
| Egg density vs. maximum NEW velocity suitability class | Class  | 2  | 0.7128  | 0.356  | 3.71 | 0.044* |  |       |   |        |        |      |        |       |    |         |        |  |       |   |        |        |      |        |       |    |         |        |  |       |   |        |        |      |        |       |    |         |        |  |       |   |        |        |      |        |       |    |         |        |  |       |   |        |        |      |        |       |    |         |        |                                       |       |   |        |        |      |        |       |    |        |        |                                       |       |   |        |        |      |        |       |    |        |        |                                       |       |   |        |        |      |        |       |    |        |        |                                       |       |   |        |        |      |        |       |
|  | Error  | 19 | 1.18276 | 0.0962 |      |        | Egg Density vs. average HSI class                      | Class | 2 | 0.318  | 0.159  | 1.4  | 0.271  | Error | 19 | 2.158   | 0.114  | Egg density vs. maximum HSI class                      | Class | 2 | 0.34   | 0.17   | 1.57 | 0.233  | Error | 20 | 2.172   | 0.109  | Egg density vs. average NEW HSI class                  | Class | 3 | 0.7206 | 0.2402 | 2.55 | 0.086  | Error | 19 | 1.7916  | 0.0943 | Egg density vs. maximum NEW HSI class                  | Class | 2 | 0.9247 | 0.4623 | 5.55 | 0.013* | Error | 19 | 1.5833  | 0.0833 |  |       |   |        |        |      |        |       |    |         |        |                                       |       |   |        |        |      |        |       |    |        |        |                                       |       |   |        |        |      |        |       |    |        |        |                                       |       |   |        |        |      |        |       |    |        |        |                                       |       |   |        |        |      |        |       |
| Egg Density vs. average HSI class                      | Class  | 2  | 0.318   | 0.159  | 1.4  | 0.271  |  |       |   |        |        |      |        |       |    |         |        |  |       |   |        |        |      |        |       |    |         |        |  |       |   |        |        |      |        |       |    |         |        |  |       |   |        |        |      |        |       |    |         |        |  |       |   |        |        |      |        |       |    |         |        |                                       |       |   |        |        |      |        |       |    |        |        |                                       |       |   |        |        |      |        |       |    |        |        |                                       |       |   |        |        |      |        |       |    |        |        |                                       |       |   |        |        |      |        |       |
|  | Error  | 19 | 2.158   | 0.114  |      |        | Egg density vs. maximum HSI class                      | Class | 2 | 0.34   | 0.17   | 1.57 | 0.233  | Error | 20 | 2.172   | 0.109  | Egg density vs. average NEW HSI class                  | Class | 3 | 0.7206 | 0.2402 | 2.55 | 0.086  | Error | 19 | 1.7916  | 0.0943 | Egg density vs. maximum NEW HSI class                  | Class | 2 | 0.9247 | 0.4623 | 5.55 | 0.013* | Error | 19 | 1.5833  | 0.0833 |  |       |   |        |        |      |        |       |    |         |        |  |       |   |        |        |      |        |       |    |         |        |                                       |       |   |        |        |      |        |       |    |        |        |                                       |       |   |        |        |      |        |       |    |        |        |                                       |       |   |        |        |      |        |       |    |        |        |                                       |       |   |        |        |      |        |       |
| Egg density vs. maximum HSI class                      | Class  | 2  | 0.34    | 0.17   | 1.57 | 0.233  |  |       |   |        |        |      |        |       |    |         |        |  |       |   |        |        |      |        |       |    |         |        |  |       |   |        |        |      |        |       |    |         |        |  |       |   |        |        |      |        |       |    |         |        |  |       |   |        |        |      |        |       |    |         |        |                                       |       |   |        |        |      |        |       |    |        |        |                                       |       |   |        |        |      |        |       |    |        |        |                                       |       |   |        |        |      |        |       |    |        |        |                                       |       |   |        |        |      |        |       |
|  | Error  | 20 | 2.172   | 0.109  |      |        | Egg density vs. average NEW HSI class                  | Class | 3 | 0.7206 | 0.2402 | 2.55 | 0.086  | Error | 19 | 1.7916  | 0.0943 | Egg density vs. maximum NEW HSI class                  | Class | 2 | 0.9247 | 0.4623 | 5.55 | 0.013* | Error | 19 | 1.5833  | 0.0833 |  |       |   |        |        |      |        |       |    |         |        |  |       |   |        |        |      |        |       |    |         |        |  |       |   |        |        |      |        |       |    |         |        |                                       |       |   |        |        |      |        |       |    |        |        |                                       |       |   |        |        |      |        |       |    |        |        |                                       |       |   |        |        |      |        |       |    |        |        |                                       |       |   |        |        |      |        |       |
| Egg density vs. average NEW HSI class                  | Class  | 3  | 0.7206  | 0.2402 | 2.55 | 0.086  |  |       |   |        |        |      |        |       |    |         |        |  |       |   |        |        |      |        |       |    |         |        |  |       |   |        |        |      |        |       |    |         |        |  |       |   |        |        |      |        |       |    |         |        |  |       |   |        |        |      |        |       |    |         |        |                                       |       |   |        |        |      |        |       |    |        |        |                                       |       |   |        |        |      |        |       |    |        |        |                                       |       |   |        |        |      |        |       |    |        |        |                                       |       |   |        |        |      |        |       |
|  | Error  | 19 | 1.7916  | 0.0943 |      |        | Egg density vs. maximum NEW HSI class                  | Class | 2 | 0.9247 | 0.4623 | 5.55 | 0.013* | Error | 19 | 1.5833  | 0.0833 |  |       |   |        |        |      |        |       |    |         |        |  |       |   |        |        |      |        |       |    |         |        |  |       |   |        |        |      |        |       |    |         |        |  |       |   |        |        |      |        |       |    |         |        |                                       |       |   |        |        |      |        |       |    |        |        |                                       |       |   |        |        |      |        |       |    |        |        |                                       |       |   |        |        |      |        |       |    |        |        |                                       |       |   |        |        |      |        |       |
| Egg density vs. maximum NEW HSI class                  | Class  | 2  | 0.9247  | 0.4623 | 5.55 | 0.013* |  |       |   |        |        |      |        |       |    |         |        |  |       |   |        |        |      |        |       |    |         |        |  |       |   |        |        |      |        |       |    |         |        |  |       |   |        |        |      |        |       |    |         |        |  |       |   |        |        |      |        |       |    |         |        |                                       |       |   |        |        |      |        |       |    |        |        |                                       |       |   |        |        |      |        |       |    |        |        |                                       |       |   |        |        |      |        |       |    |        |        |                                       |       |   |        |        |      |        |       |
|  | Error  | 19 | 1.5833  | 0.0833 |      |        |  |       |   |        |        |      |        |       |    |         |        |  |       |   |        |        |      |        |       |    |         |        |  |       |   |        |        |      |        |       |    |         |        |  |       |   |        |        |      |        |       |    |         |        |  |       |   |        |        |      |        |       |    |         |        |                                       |       |   |        |        |      |        |       |    |        |        |                                       |       |   |        |        |      |        |       |    |        |        |                                       |       |   |        |        |      |        |       |    |        |        |                                       |       |   |        |        |      |        |       |

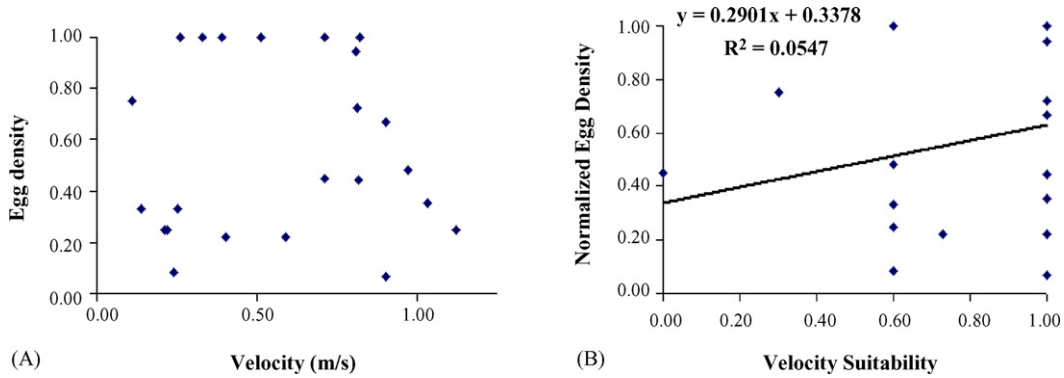


**Fig. 5 – Relationship of normalized egg densities to the (A) average velocities experienced. (B) The relationship between normalized egg density and the average velocity suitability experienced.**

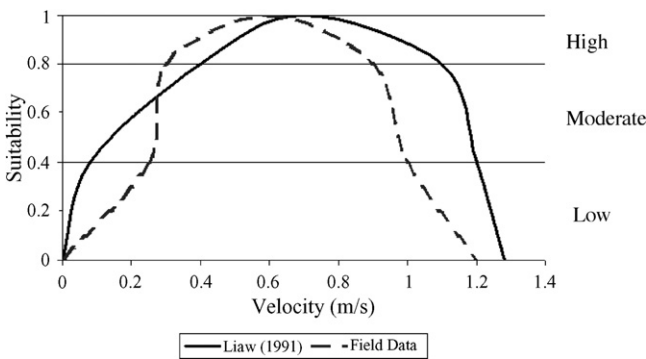


**Fig. 6 – Comparison of the suitability curve from Liaw (1991) and the one derived from the field and model data. Horizontal lines show the cutoff values for the different suitability classes (low, moderate, and high).**

in Fig. 5A. A relationship between these two variables is visible with all of the maximum egg densities occurring between velocities of 0.3 and 0.95 m/s. A curve was fitted to these data and used as a new velocity suitability relationship (Fig. 6). The HSI outputs using this new curve were compared with those from the original curves. No significant correlation between normalized egg density and the average velocity suitability

before collection was found using the suitability curve from the Saskatchewan Fisheries Laboratory (Fig. 5B). ANOVA comparisons of normalized egg density and the average velocity suitability classes observed before collection revealed no significant differences between the classes (Table 3).

There was no significant correlation between normalized egg densities and the average HSI experienced before collection using the velocity suitability curve from the literature (Fig. 7A). However, when the velocity suitability curve constructed from the field data was used the correlation became significant ( $P = 0.036$ , Table 3) (Fig. 7B). ANOVA comparisons of normalized egg density between the average HSI classes using both the literature and field data velocity suitability curves failed to reveal significant differences between the classes (Table 3).

**4.2. Sandusky River habitat quality**

The new velocity suitability curve was used to run the Sandusky habitat quality analysis simulations due to its more accurate depiction of habitat suitability. The results from the flood wave simulation indicate that the WUA and the amount of highly suitable habitat in this reach of the river increase rapidly with discharge and peak between 20 and 25 m<sup>3</sup>/s (Fig. 8). The values of these two indices are half of their maximum at around 55 m<sup>3</sup>/s. By 100 m<sup>3</sup>/s the amount of highly

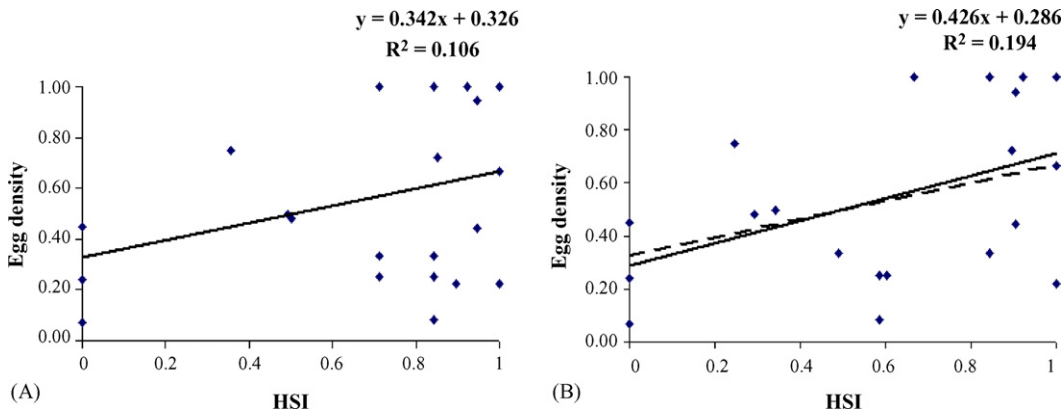


**Fig. 7 – The relationship between normalized egg density and average HSI experienced using (A) the literature and (B) the field data velocity suitability curves. The dashed line in (B) represents the linear regression in (A).**

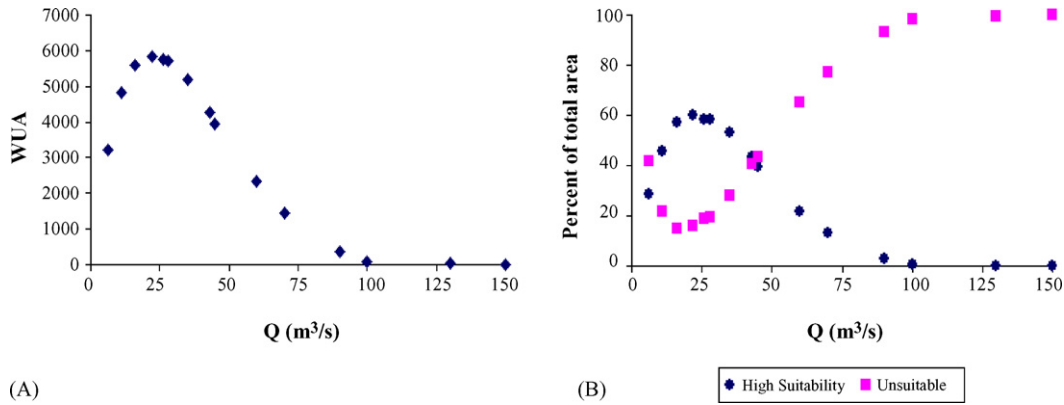


**Fig. 8 – (A) The relationship between WUA and discharge in the study area. (B) The relationship between the percent of the total habitat area in the high suitability and unsuitable classes for a given discharge.**

suitable habitat available is less than 1%, while the amount of unsuitable habitat is 98% (Fig. 8B). Fig. 9 displays HSI maps created by the model for a range of the simulated discharges. At 5 m³/s most of the unsuitable habitat falls in the fringe habitats along the shore and around the islands where it is too shallow. The main channel (displayed primarily in orange) has higher suitability due to its greater depth and appropriate velocity. At 45 m³/s, this trend becomes reversed, with the main channel becoming too deep and fast and the fringe habitats becoming more suitable. By 100 m³/s, almost the entire reach of the river becomes unsuitable.

The WUA during the spawning season can vary drastically (Fig. 10). It is clear that the length of the spawning season (determined by temperature) and the discharge during that time (represented as total volume in Fig. 10C) combine to determine the suitability of the reach. The volume of flow dur-

ing the spawning season is determined as:

$$\int_0^T Q dt \tag{5}$$

where Q is the daily discharge (m³/d) and T is the duration of the spawning season (days).

For example, in 1991, favorable discharges and a long spawning season combined to produce the highest average WUA and the second highest cumulative WUA (Fig. 10A-C). In 1990 a slightly higher cumulative WUA was obtained due to the longer season (Fig. 10C). However, in that year a large flood event occurred that drove the WUA down close to zero for a period of time, thus causing the average WUA to be lower than in 1991 (Fig. 10A and B). 1993 experienced both the lowest average and cumulative WUA due to the highest discharges

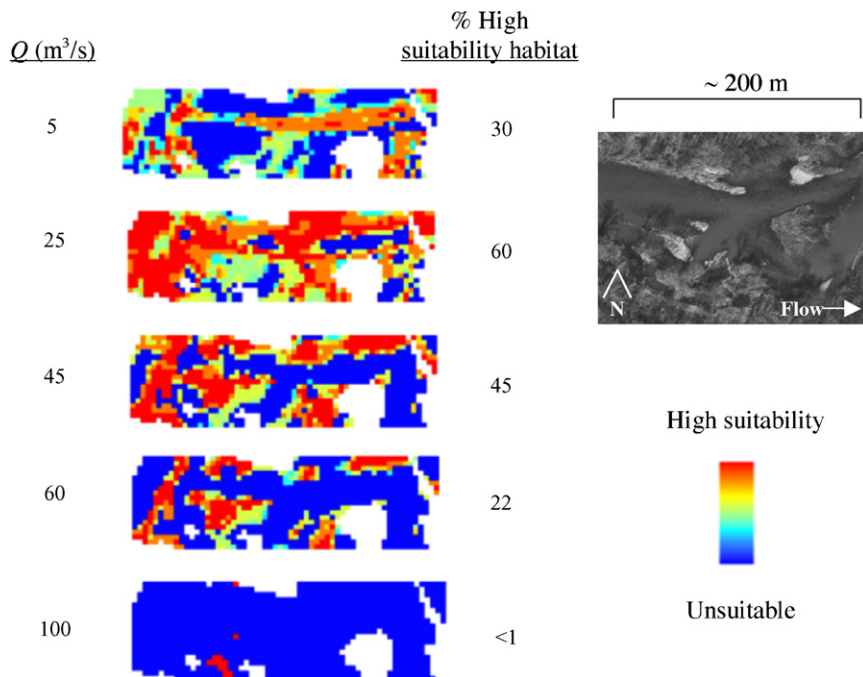


**Fig. 9 – HSI maps of the study area (shown in the inset photograph) produced by the model for a range of discharges.**

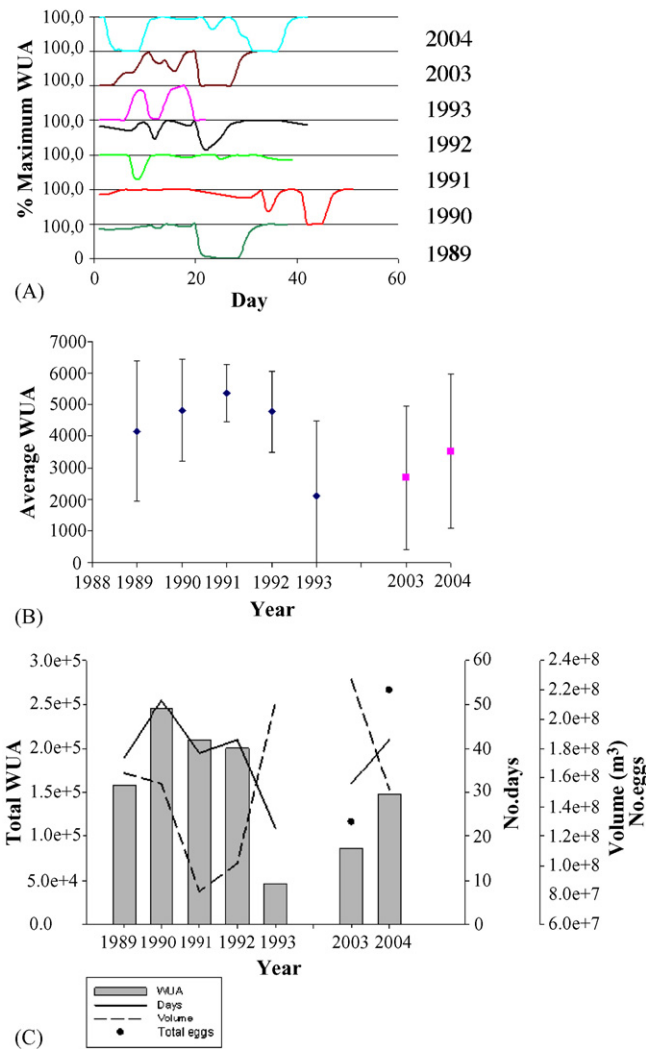


**Fig. 10 – (A) Time series of % maximum (from 0 to 100) WUA for seven spawning seasons; (B) average WUA during the seven spawning seasons ( $\pm 1$  S.D.); (C) cumulative WUA for the seven spawning seasons compared with the length of the season and volume of water flowing through the study reach. The estimated total egg deposition in 2003 and 2004 is also shown.**

occurring over the shortest spawning season (Fig. 10A–C). 2003 and 2004 seem to both fall in the lower end of the scale for both average and cumulative WUA (Fig. 10A–C). 2003 experienced higher discharges over a shorter time period, thus causing it to have lower average and cumulative WUA values (Fig. 10A–C).

## 5. Discussion

### 5.1. Evaluation of the model

The integration of a one-dimensional hydraulic model with a GIS-based HSI model worked well in many regards, but also had some shortcomings. Data transfer from the hydraulic model to the GIS was quite simple. The automation of the depth, velocity, and HSI modules allowed for a long time series

to be simulated quickly without the user having to manually set up the calculations using the ArcGIS Spatial Analyst, as is the case in most previous GIS-based HSI modeling efforts (Brown et al., 2000; Rubec et al., 1998; Tiffan et al., 2002). Also, each module creates permanent raster layers (depth, velocity, depth and velocity suitability, and HSI) for each step of the time series, which allowed analyses to be performed on each of these variables. The effectiveness of each of the GIS modules is discussed below.

The results of the model validation indicate that the GIS depth module adequately predicts depths throughout the study reach for the range of discharges sampled ( $14\text{--}46\text{ m}^3/\text{s}$ ). While there is some deviation about the mean difference between modeled and predicted depths (Table 2), this is an acceptable artifact of attempting to compare a point depth measurement in the field to a value averaged over a  $3\text{ m} \times 3\text{ m}$  cell in the model. The velocity predictions, however, were not as accurate. The model consistently underestimated velocities in the study reach for the range of discharges sampled. This could be the result of a combination of the complex channel geometry of the study reach and the fact that we were only able to collect velocity data to calibrate the model at a single discharge at the lower end of the range of validation discharges. Additional calibration data at higher discharges may have improved modeled velocities but were impractical to collect for this study using an Doppler systems for such a difficult channel. Because of heterogeneity of the riffle-pool structure in the study area, high velocities occurred in certain locations even at the moderate flow sampled for the calibration data set. Thus, the range of measured velocities for the calibration was adequate to validate the dominant features in the HSI model.

Even the simplest of natural channels can display complex flow patterns that are not adequately accounted for by standard velocity measurement field techniques (Kondolf et al., 2000). The study reach contained several areas of complex morphology leading to similarly complex velocity fields. Attempting to resolve these high resolution variations at the  $3\text{ m} \times 3\text{ m}$  grid size will lead to the loss of information and the smoothing over of small scale differences in velocity (Leclerc et al., 1994, cited in Leclerc et al., 1996). The fact that our validation velocity measurements were done at the points where egg samples were taken resulted in the comparison of a single point velocity to a velocity estimated from the average characteristics (depth, roughness, substrate) of a  $9\text{ m}^2$  area. Decreasing the cell size to resolve these differences would have created artificially higher topographic resolution with unknown certainty and was, therefore, not attempted.

Manning's  $n$  was calibrated at a lower discharge, and hence lower depths, than most of the validation datasets which presents a problem, since the Manning's  $n$  generally decreases with increasing depth. However, this change is not uniform (Julien, 2002). A depth-correlated correction factor was applied to the Manning's  $n$  values, but this did not increase the accuracy of the model due to the non-uniform change of roughness with depth throughout the study area. Since discharges were greater during the collection of validation data than the discharge during the collection of the calibration data, it is likely that the Manning's coefficient used in the model was too large at the higher water levels, causing the velocity to be underesti-

mated. Despite these problems, the model accurately predicts first order velocity distributions across the study reach (i.e., relative high and low velocities are predicted in areas where they were observed in the field on a given sampling day).

Many researchers have begun using two-dimensional hydraulic models in HSI modeling and have described their superiority over traditional one-dimensional methods (Ghanem et al., 1996; Leclerc et al., 1996; Tiffan et al., 2002; Bockelmann et al., 2004; Korman et al., 2004). One of the major benefits of two-dimensional models is that they do not rely on the collection of several high resolution *in situ* water velocity datasets to accurately predict velocities at other discharges. Also, two-dimensional models better account for the lateral and downstream transfer of fluid mass and momentum, making their velocity predictions more realistic in magnitude and direction than those of most one-dimensional models (Kondolf et al., 2000). However, these more advanced methods may still have difficulty predicting velocity distributions in areas with complex channel geometry, even if high resolution bed topography data are available to create a detailed computational grid (Pasternack et al., 2004). There are many variables that influence water movement that are not accounted for in hydraulic models. Neither one- or two-dimensional hydraulic models are sophisticated enough to accurately describe the physics of the flow fields found in complex channels (Kondolf et al., 2000). Regardless of this shortcoming, two-dimensional models are rapidly becoming the industry standard, and it is likely that there will be a reduction in the use of the more primitive one-dimensional methods in HSI modeling.

Despite the fact that the model was most accurate at predicting depths, the depths showed the weakest correlation with egg densities (Fig. 4). The researchers that constructed the suitability curves used in this study noted that depth displayed the weakest relationship with egg densities of the three habitat variables and indicate that it is most likely only used by walleye for habitat selection once velocity and substrate criteria are met (Liaw, 1991). Also, since most of our egg samples were located in areas that experienced depths between 20 and 80 cm before collection (and at the time of sampling), it is difficult to make comparisons between extremely shallow and deep areas. Suitability curves constructed on data from larger rivers in Western America indicate that walleye will spawn in depths of up to 1.9 m (McMahon and Terrell, 1984). It is, therefore, likely that the water depths for the validation dataset were not extreme enough to influence habitat selection.

The relationship between egg density and velocity is more obvious. The construction of a new rudimentary velocity suitability curve to fit these data resulted in a significant correlation between HSI and egg density (Fig. 7). The new velocity suitability curve was similar to the original (Fig. 6), but caused a significant change in the model's ability to predict egg densities. This indicates the importance of having accurate suitability curves for the river being studied. Curves developed in a different system, regardless of how similar the two systems are, may not be appropriate. When possible, suitability curves should be constructed for the river in question (Bovee et al., 1998). However, doing this correctly requires a great deal of time and effort and may not be possible within the constraints of the project.

The spawning behavior of walleye is a complex ritual (Ellis and Giles, 1965), which is undoubtedly influenced by other factors, both biotic and abiotic, which are not accounted for by the simple mathematical relationship of an HSI model (Mathur et al., 1985; Lowie et al., 2001). Also, the fact that walleye are broadcast spawners indicates that eggs spawned in one location may be flushed into other areas with different suitability values, making it difficult to determine where the eggs were originally meant to be deposited. Despite the low  $R^2$  values, the correlation between egg density and the average HSI is significant. The relationship indicates an increase in egg density with increasing HSI, which is what would be expected. Therefore, despite the shortcomings of the model, we feel that it is able to give an adequate representation of the variation in spawning habitat suitability in this reach of the Sandusky River.

## 5.2. Habitat suitability dynamics in the Sandusky River

The habitat suitability in the study reach changes dramatically with discharges ranging from 5 to 100 m<sup>3</sup>/s. Habitat suitability is maximized between 20 and 25 m<sup>3</sup>/s while flood events with discharges of over 100 m<sup>3</sup>/s, which are not uncommon in early spring, can drive the WUA to almost zero (Fig. 8). In both 2003 and 2004, the early part of the spawning season was dominated by high discharge flood events, which prevented sampling (Fig. 10A). Samples taken the first few days after these events in both years did not contain any eggs in advanced stages of development, indicating that either no spawning had taken place during the flood or that eggs deposited before or during the flood had been flushed out of the gravel substrate and presumably deposited downstream in slower-moving areas of poorer quality habitat (sand/mud substrate). In 2004, however, samples following a second flood event of over 100 m<sup>3</sup>/s contained several eggs in late developmental stages, which could mean that eggs are not easily flushed out of the substrate and that spawning simply does not take place during high discharges. Either way, it is likely that years with several flood events during the spawning season will experience lower reproductive success than those with consistent, moderate discharge. This is evident in the 2003 and 2004 data. 2003, a year with a shorter spawning season with several flood events, had almost half of the total egg deposition that was estimated for 2004 (Fig. 10C).

The apparent dependence of habitat suitability on discharge has implications for the Sandusky River walleye population. Gravel habitat is scarce in the river with only one major bed of approximately 64 000 m<sup>2</sup> in area. A year with poor habitat suitability in this area of the river could lead to low reproductive success and thus a poor year class. If walleye had access to other areas of gravel habitat further upstream, they may be able to find a more suitable spawning area during flood events. No two-dimensional HSI modeling has been performed in the upstream areas, however, so it is unknown if these habitats will be similarly impacted by flood events affecting the below-dam area. Such an action could help to guide ecosystem restoration activities on this river, and add useful information for making a decision on the fate of the Ballville Dam.

Models of spawning and early life history stages in the Sandusky River by two independent groups both indicated that removing the Ballville Dam and allowing walleye to migrate to upstream gravel beds would greatly increase the amount of larvae produced in the river (Jones et al., 2003; Cheng et al., 2006). However, the results of Gillenwater (2005) show that simply increasing the amount of habitat in the Sandusky River via restoration practices would not be enough to increase larval production due to the apparent lack of habitat limitation in the system. Neither of the models take fine scale differences in habitat suitability into account, so it is difficult to determine if these upstream areas will offer patches of suitable habitat that could be utilized during flood events. Coupling an HSI model with population models similar to those by Jones et al. (2003) and Cheng et al. (2006) would make the connection between habitat suitability dynamics and reproductive success and give a more accurate description of how the walleye population could benefit from dam removal.

The apparent dependence of reproductive success on river discharge has further reaching implications for landscape-scale processes. Before the arrival of European settlers, the Sandusky Watershed was dominated by forests and extensive wetlands (SRWC, 2002). Row crop agriculture now makes up 82% of the land use in the watershed with forests and wetlands comprising a meager 15% (SRWC, 2002), a change which has likely altered the hydrology of the river. The conversion of riparian forests and wetlands to agriculture and the installation of drainage tiles to rapidly move water from the fields to waterways are actions known to cause an increase in the magnitude of flood events. Storm sewer drainage from the cities of Fremont and Tiffin and other smaller municipalities bordering the river will also have contributed to this effect. The relationship between river behavior and watershed characteristics underscores the fact that river restoration activities must take place on a landscape scale, not just within the channel (Clarke et al., 2003). In the case of walleye spawning, the addition of more gravel habitat to the river may not increase reproductive success very much, if the hydraulic conditions are still unsuitable.

## 6. Conclusions

Environmental management decision making requires the most complete and accurate information possible, especially when the issue at hand is as politically charged as the proposed removal of the Ballville Dam on the Sandusky River. HSI models can be useful tools in this process by adding information about the current or potential future habitat conditions. For these models to be effective, they must be reliable and readily available to organizations that need them. The model presented in this work could be useful because it is nested within ArcGIS, the most popular commercial GIS software on the market. The model also easily interfaces with the output from any one-dimensional hydraulic river model. The HSI predictions displayed a significant positive correlation with egg densities in the study reach. However, the model has difficulty predicting velocity distributions in channels with complex morphology, which unfortunately is often the type of area that needs to be modeled. The use of a two-dimensional hydraulic

model to predict depth and velocity distributions instead of performing the calculations within the GIS could potentially provide more accurate results.

Even with such a change, it may still be the fact that walleye spawning behavior simply does not conform to the HSI relationship as well as hoped. Ecological phenomena are far more complex than a simple mathematical expression and the predictions of HSI models should only be considered as approximations of reality. Therefore, the results of such models must be weighed against their assumed accuracy when being used in the decision making process.

## Acknowledgements

The authors thank Randy Sanders, Gary Isbell, Roger Knight, Dick Bartz and Keith Banachowski (Ohio Department of Natural Resources) for their interest in this project; to Connie Livchak and Ryan Murphy (Geological Survey, ODNR) for their data on surface substrate distributions; and to Michael Eberle (U.S. Geological Survey) for providing historical water data. We also thank members of our group, Fang Cheng, Chris Tomsic, and David Davis, for their help with modeling and fieldwork. Finally, the authors are indebted to Roy Stein and Aquatic Ecology Laboratory (OSU), the reviewers and editors for early suggestions that improved the manuscript. This research was supported by a grant from the Great Lakes Protection Fund, no. 671.

## REFERENCES

- Arcement, G., Schneider, V., 1989. Guide for selecting Manning's roughness coefficients for natural channels and flood plains. U.S. Geological Survey water supply paper no. 2339.
- Armstrong, J., Dyke, R., 1967. Walleye egg deposition on artificial spawning beds constructed in the Otonabee River at Bobcaygeon. Ontario Department of Lands and Forests. Report # 91.
- Bannister, A., Raymond, S., Baker, R., 1998. Surveying, 7th ed. Addison Wesley Longman Ltd., Harlow, UK, 502 pp.
- Bockelmann, B.N., Fenrich, E.K., Lin, B., Falconer, R.A., 2004. Development of an ecohydraulics model for stream and river restoration. *Ecol. Eng.* 22, 227–235.
- Bovee, K., Lamb, B., Bartholow, J., Stalnaker, C., Taylor, J., Henriksen, J., 1998. Stream habitat analysis using the Instream Flow Incremental Methodology. U.S. Geological Survey Information and Technology Report USGS/BRD-1998-0004. Fort Collins, CO: USGS Biological Resources Division.
- Bovee, K., Milhous, R., 1978. Hydraulic simulation in instream flow studies: theory and techniques. Instream flow information paper no. 5. U.S. Fish and Wildlife service.
- Brown, S., Buja, K., Jury, S., Monaco, M., 2000. Habitat suitability index modeling for eight fish and invertebrate species in Casco and Sheepscot Bays, Maine. *N. Am. J. Fish. Manage.* 20, 408–435.
- Chapra, S.H., 1997. Surface Water Quality Modeling. McGraw-Hill Press, NY, p. 784.
- Cheng, F., 2001. Modeling effects of dam removal on migratory walleye life stages in a coastal watershed. M.S. Thesis. The Ohio State University, Columbus.
- Cheng, F., Zika, U., Banachowski, K., Gillenwater, D., Granata, T., 2006. Modelling the effects of dam removal on migratory walleye (*Sander vitreus*) early life-history stages. *River Res.*

- Appl. 22 (8), doi:10.1002/rra.939 <http://www3.interscience.wiley.com/cgi-bin/jhome/90010544>.
- Clarke, S., Bruce-Burgess, L., Wharton, G., 2003. Linking form and function: towards an eco-hydromorphic approach to river restoration. *Aquat. Conserv.: Mar. Freshwater Syst.* 13, 439–450.
- Crowe, W., 1962. Homing behavior in walleyes. *Trans. Am. Fish. Soc.* 91, 350–354.
- Eastwood, P., Meaden, G., Grioche, A., 2001. Modeling spatial variation in spawning habitat suitability for the sole *Solea solea* using regression quantiles and GIS procedures. *Mar. Ecol. Prog. Ser.* 224, 251–266.
- Ellis, D.V., Giles, M.A., 1965. The spawning behavior of the Walleye *Stizostedion vitreum* (Mitchill). *Trans. Am. Fish. Soc.* 94, 358–362.
- Environment Canada and U.S. EPA, 2002. Lake Erie lakewide management plan. 2002 update. <http://www.epa.gov/glnpo/lakeerie/>.
- Eschmeyer, P., 1950. The life history of the walleye (*Stizostedion vitreum*) (Mitchill) in Michigan. Michigan Department of Conservation, Institute of Fisheries research bulletin no. 3.
- Fisher, W., Rahel, F., 2004. Geographic information systems applications in stream and river fisheries. In: Fisher, W., Rahel, F. (Eds.), *Geographic information systems applications in stream and river fisheries*. Geographic Information Systems in Fisheries. American Fisheries Society, MA, 275 pp.
- Fluhart, D., 2000. Habitat protection, ecological issues, and implementation of the sustainable fisheries act. *Ecol. Appl.* 10, 325–337.
- Ghanem, A., Steffler, P., Hicks, F., Katopodis, C., 1996. Two-dimensional hydraulic simulation of physical habitat conditions in flowing streams. *Regul. Rivers: Res. Manage.* 12, 185–200.
- Gillenwater, D.A., 2005. Modeling walleye (*Sander vitreus*) spawning habitat suitability and reproductive success in the Sandusky River (Ohio, USA). M.S. Thesis. The Ohio State University, Columbus.
- Jennings, M., Claussen, J., David, P., 1996. Evidence for heritable preferences for spawning habitat between two walleye populations. *Trans. Am. Fish. Soc.* 125, 978–982.
- Jones, M., Netto, J., Stockwell, J., Mion, J., 2003. Does the value of newly accessible spawning habitat for walleye (*Stizostedion vitreum*) depend on its location relative to nursery habitats? *Can. J. Fish. Aquat. Sci.* 60, 1527–1538.
- Julien, R.P., 2002. *River Mechanics*. Cambridge University Press, Cambridge, UK, 434 pp.
- Kondolf, G.M., Larsen, E.W., Williams, J.G., 2000. Measuring and modeling the hydraulic environment for assessing instream flows. *N. Am. J. Fish. Manage.* 20, 1016–1028.
- Korman, J., Wiele, S.M., Torizzo, M., 2004. Modelling effects of discharge on habitat quality and dispersal of juvenile humpback chub (*Gila cypha*) in the Colorado River, Grand Canyon. *River Res. Appl.* 20, 379–400.
- Langton, R.W., Steneck, R.S., Gotceitas, V., Juanes, F., Lawton, P., 1996. The interface between fisheries research and habitat management. *N. Am. J. Fish. Manage.* 16, 1–7.
- Leach, J., Nepszy, S., 1976. The fish communities of Lake Erie. *J. Fish. Res. Board Can.* 33, 622–638.
- Leclerc, M., Boudreau, P., Bechara, J., Belzile, L., Villeneuve, D., 1994. Modélisation de la dynamique de l'habitat des ouananiches (*Salmo salar*) juvéniles de la rivière Ashuapmushan (Québec, Canada). *Bull. Fr. Pechet Pisciculture* 332, 11–32, as cited in Leclerc et al. (1996).
- Leclerc, M., Boudreau, P., Berchara, J., Belzile, L., 1996. Numerical method for modeling spawning habitat dynamics of landlocked salmon, *Salmo salar*. *Regul. Rivers: Res. Manage.* 12, 273–285.
- Liaw, W., 1991. Habitat suitability criteria for walleye spawning and egg incubation in Saskatchewan. Saskatchewan Fisheries Laboratory. Fisheries Technical Report 91-1.
- Lowie, C.E., Haynes, J.M., Walter, R.P., 2001. Comparison of walleye habitat suitability index (HSI) information with habitat features of a walleye spawning stream. *J. Freshwater Ecol.* 16, 621–632.
- Mathur, D., Bason, W., Purdy Jr., E., Silver, C., 1985. A critique of the instream flow incremental methodology. *Can. J. Fish. Aquat. Sci.* 42, 825–830.
- McElman, J., Balon, E., 1979. Early ontogeny of walleye, *Stizostedion vitreum*, with steps of salutatory development. *Environ. Biol. Fish.* 4, 309–348.
- McMahon, T., Terrell, J., 1984. Habitat suitability information: walleye. US Fish and Wildlife Service. FWS/OBS-82/10.56.
- Merker, R., Woodruff, R., 1996. Molecular evidence for divergent breeding groups of walleye (*Stizostedion vitreum*) in tributaries to Western Lake Erie. *J. Great Lakes Res.* 22, 280–288.
- NOAA/NOS (National Oceanographic and Atmospheric Administration/National Oceanographic Service) Historic Great Lakes Water Level Data (Station 9063079), [http://tidesandcurrents.noaa.gov/station\\_retrieve.shtml?type=Historic+Great+Lakes+Water+Level+Data/](http://tidesandcurrents.noaa.gov/station_retrieve.shtml?type=Historic+Great+Lakes+Water+Level+Data/). Accessed 2004 December 1.
- Pasternack, G.B., Wang, C.L., Merz, J.E., 2004. Application of a 2D hydrodynamic model to design of reach-scale spawning gravel replenishment on the Mokelumne River, California. *River Res. Appl.* 20, 205–225.
- Regier, H., Applegate, V., Ryder, R., 1969. The ecology and management of the walleye in Western Lake Erie. Great Lakes Fishery Commission, Technical Report # 15.
- Rosenfeld, J., 2003. Assessing the habitat requirements of stream fishes: an overview and evaluation of different approaches. *Trans. Am. Fish. Soc.* 132, 953–968.
- Rowe, D.K., Shankar, U., James, M., Waugh, B., 2002. Use of GIS to predict effects of water level on the spawning area for smelt, *Retropinna retropinna*, in Lake Taupo, New Zealand. *Fish. Manage. Ecol.* 9, 205–216.
- Rubec, P., Coyne, M., McMichael, R., Monaco, M., 1998. Spatial models being developed in Florida to determine essential fish habitat. *Fisheries* 20, 21–25.
- Spence, R., Hickley, P., 2000. The use of PHABSIM in the management of water resources and fisheries in England and Wales. *Ecol. Eng.* 16, 153–158.
- SRWC (Sandusky River Watershed Coalition), 2002. Resource inventory. July 31, 2003. [http://www.riverwatershed.org/srwc/res\\_inven/](http://www.riverwatershed.org/srwc/res_inven/).
- Stepaniuk, J., 1989. Walleye (*Stizostedion vitreum*) utilization and reproductive success on habitat enhancement sites within the Whiteshell Provincial Park, 1987. Manitoba Department of Natural Resources, Fisheries Branch Report # 89-10.
- Tea, V., 1999. Sandusky River walleyes. What does the future hold? *Wild Ohio Magazine*. Ohio Department of Natural Resources. <http://www.dnr.ohio.gov/wildlife/Resources/wildohio/wildohio.htm>.
- Tiffan, K., Garland, R., Rondolf, D., 2002. Quantifying flow dependent changes in subyearling fall Chinook salmon rearing habitat using two-dimensional spatially explicit modeling. *N. Am. J. Fish. Manage.* 22, 713–726.
- USFWS (U.S. Fish and Wildlife Service), 1980. Habitat as a basis for environmental assessment. USFWS. Report 101 ESM, Fort Collins, CO.
- Waddle, T.J. (Ed.), 2001. PHABSIM for Windows: User's Manual and Exercises. U.S. Geological Survey, Fort Collins, CO, 288 pp.